JCI The Journal of Clinical Investigation

Dose intensification of TRAIL-inducing ONC201 inhibits metastasis and promotes intratumoral NK cell recruitment

Jessica Wagner, … , Mark N. Stein, Wafik El-Deiry

J Clin Invest. 2018. https://doi.org/10.1172/JCI96711.

Research Article In-Press Preview **Oncology**

ONC201 is a first-in-class, orally active anti-tumor agent that upregulates cytotoxic TRAIL pathway signaling in cancer cells. ONC201 has demonstrated safety and preliminary efficacy in the first-in-human trial where patients were dosed every 3 weeks. We hypothesized that dose-intensification of ONC201 may impact anti-tumor efficacy. We discovered that ONC201 exerts dose- and schedule-dependent effects on tumor progression and cell-death signaling in vivo. With dose intensification, we note a potent anti-metastasis effect and inhibition of cancer cell migration and invasion. Our preclinical results prompted a change in ONC201 dosing in all open clinical trials. We observe accumulation of activated NK+ and CD3+ cells within ONC201-treated tumors, and NK-cell depletion inhibits ONC201 efficacy in vivo, including against TRAIL/ONC201-resistant *Bax*$^{-/-}$ tumors. Immunocompetent NCR1-GFP mice with GFP-expressing NK-cells demonstrate GFP(+)-NK cell infiltration of syngeneic MC38 colorectal tumors. Activation of primary human NK cells and increased degranulation occur in response to ONC201. Co-culture experiments identified a role for TRAIL in human NK-mediated anti-tumor cytotoxicity. Preclinical results indicate potential utility for ONC201 plus anti-PD-1 therapy. We observed an increase in activated TRAIL-secreting NK cells in the peripheral blood of patients after receiving ONC201 treatment. The results offer a unique pathway of immune stimulation for cancer therapy.

Dose-intensification of TRAIL-inducing ONC201 inhibits metastasis and promotes intratumoral NK cell recruitment

Jessica Wagner[1], C. Leah Kline[1], Lanlan Zhou[1], Kerry S. Campbell[2], Alexander W. MacFarlane[2], Anthony J. Olszanski[3], Kathy Q. Cai[4], Harvey H. Hensley[5], Eric A. Ross[6], Marie D. Ralff[1], Andrew Zloza[7], Charles B. Chesson[7], Jenna H. Newman[7], Howard Kaufman[7], Joseph Bertino[7], Mark Stein[7] and Wafik S. El-Deiry[1,*]

[1]Laboratory of Translational Oncology and Experimental Cancer Therapeutics, Molecular Therapeutics Program and Department of Hematology/Oncology, Fox Chase Cancer Center, Philadelphia, PA, 19111, USA
[2]Blood Cell Development and Function Program, Institute for Cancer Research, Fox Chase Cancer Center, Philadelphia, PA, 19111, USA.
[3]Department of Hematology/Oncology and Molecular Therapeutics Program, Fox Chase Cancer Center, Philadelphia, PA, 19111, USA
[4]Histopathology Facility, Fox Chase Cancer Center, Philadelphia, PA, 19111, USA.
[5] Biological Imaging Facility, Fox Chase Cancer Center; Philadelphia, PA, 19111, USA.
[6]Biostatistics and Bioinformatics Facility, Fox Chase Cancer Center; Philadelphia, PA, 19111, USA.
[7]Rutgers Cancer Institute of New Jersey, New Brunswick, NJ, 08903, USA

Key words: ONC201; natural killer cell; cancer therapy; metastasis; dose intensification, CXCL10, IFN-alpha

One Sentence Summary: ONC201 exerts immune and anti-metastasis effects

*Correspondence: Wafik S. El-Deiry, Fox Chase Cancer Center, 333 Cottman Ave, P2035, Philadelphia PA, 19111. Tel: 215-214-4233; email: wafik.eldeiry@fccc.edu

Abstract

ONC201 is a first-in-class, orally active anti-tumor agent that upregulates cytotoxic TRAIL pathway signaling in cancer cells. ONC201 has demonstrated safety and preliminary efficacy in the first-in-human trial where patients were dosed every 3 weeks. We hypothesized that dose-intensification of ONC201 may impact anti-tumor efficacy. We discovered that ONC201 exerts dose- and schedule-dependent effects on tumor progression and cell-death signaling in vivo. With dose intensification, we note a potent anti-metastasis effect and inhibition of cancer cell migration and invasion. Our preclinical results prompted a change in ONC201 dosing in all open clinical trials. We observe accumulation of activated NK+ and CD3+ cells within ONC201-treated tumors, and NK-cell depletion inhibits ONC201 efficacy in vivo, including against TRAIL/ONC201-resistant *Bax*$^{-/-}$ tumors. Immunocompetent NCR1-GFP mice with GFP-expressing NK-cells demonstrate GFP(+)-NK cell infiltration of syngeneic MC38 colorectal tumors. Activation of primary human NK cells and increased de-granulation occur in response to ONC201. Co-culture experiments identified a role for TRAIL in human NK-mediated anti-tumor cytotoxicity. Preclinical results indicate potential utility for ONC201 plus anti-PD-1 therapy. We observed an increase in activated TRAIL-secreting NK cells in the peripheral blood of patients after receiving ONC201 treatment. The results offer a unique pathway of immune stimulation for cancer therapy.

Introduction

We previously identified small molecule ONC201/TIC10 that upregulates endogenous TNF-Related Apoptosis-Inducing Ligand (TRAIL), in tumor and normal cells, restoring autocrine and paracrine anti-tumor activity within tumor cells (1). The search for TRAIL-inducing compounds (TIC's) was specifically aimed at identifying compounds that do not rely on p53, leading to the discovery of ONC201/TIC10. The novel anti-cancer therapeutic ONC201 upregulates the endogenous TRAIL expression through dual blockade of Akt and ERK that releases Foxo3a to enter the nucleus and transcriptionally activate the *TRAIL* gene (1). Our prior work using shTRAIL and RIK-2 (a TRAIL-blocking antibody) demonstrated the relevance of TRAIL to the mechanism of action of ONC201 (1-3). As we investigated the kinetics of cell death we discovered that at early time points ONC201 activates the integrated stress response, inducing eIF2-alpha-dependent ATF4 and CHOP and increasing TRAIL death receptor 5 (DR5) expression (4-6). We also recently demonstrated potent anti-tumor effects on colorectal cancers initiated by cancer stem/progenitor cells (CSCs) (7). In vivo, first-in-class small molecule ONC201 possesses a broad spectrum of anti-cancer activity, a wide safety margin, robust stability, aqueous solubility, blood-brain barrier penetration, and favorable pharmacokinetics (1-5, 7-14).

Prior evidence has demonstrated that TRAIL can inhibit cancer metastasis (15-18). Inactivating mutations in the *TRAIL-R1* and *TRAIL-R2* genes have been observed in metastases in several tumor types, including mammary tumors and melanoma (19, 20). The TRAIL pathway is part of the innate host immune surveillance mechanism against cancer and involves activation of the extrinsic cell death pathway selectively in cancer cells. As part of the immune system, natural killer (NK) cells respond to cellular signals that can trigger their activation, releasing perforins and granzymes, inducing cellular lysis within the tumor. In addition, NK cells secrete TRAIL and produce cytokines including interferon gamma (IFNγ) that promote apoptosis in tumor cells and recruit other immune-like cells (21-23).

The therapeutic promise of ONC201 in preclinical in vivo studies in solid tumors, hematological malignancies, and cancer stem cells prompted its ongoing clinical development. In Phase I clinical testing with ONC201, patients, including those with prostate cancer, were treated every 3 weeks and the drug showed safety and promising efficacy in multiple tumor types (13, 24). The recommended phase II dose (RP2D) of ONC201 was determined to be 625 mg given orally every 3 weeks to patients with advanced cancer (24).

To maximize the clinical benefits of ONC201 and further elucidate its mechanism of action, we investigate here the impact of dose-intensification on ONC201's anti-tumor efficacy, unravel its anti-metastasis properties and ability to induce an immune response leading to tumor growth suppression. Through the use of syngeneic mouse models, co-culture of established human NK and tumor cells, primary normal and cancer patient NK cell data we have uncovered an unanticipated immune stimulatory anti-tumor effect of ONC201 involving natural killer (NK) and T cells along with a potent anti-metastasis effect. We further explored the mechanism to identify that TRAIL plays a role in both ONC201-anti metastasis and ONC201-induced NK cell cytotoxicity. Finally, we identify key chemokines and cytokines that are upregulated by ONC201 treatment. We explored the consequences of NK cell depletion in vivo and in preliminary experiments the prospects of combining ONC201 with anti-PD1 therapy. Our findings reveal novel aspects of the mechanism of action of anti-tumor compound ONC201 including insights into its anti-metastasis and pro-immune response activity, and potentially more efficacious dosing regimens for the drug in clinical trials.

Results

ONC201 dose intensification negatively impacts tumor growth and metastasis

Given that every 3-week ONC201 dosing was well-tolerated in the clinic, we explored the potential to augment its anti-tumor efficacy through dose-intensification in preclinical models. We found that dose-intensification of ONC201 significantly increases the extent of tumor growth inhibition in colorectal HCT116 *p53*$^{-/-}$, HT29, and breast MDA-MB-231 human tumor xenografts (Figure 1a-c, SFigure 1a-c, f). Doses of 50 mg/kg and 100 mg/kg impact primary tumor growth in a drug administration frequency-dependent manner in the aggressive HT29 xenograft (SFigure 1e). Importantly, some tumors are completely ablated after 100 mg/kg weekly dosage for a month in HCT116 *p53*$^{-/-}$ or MDA-MB-231 tumor-bearing mice (SFigure 1a, c). In mice, we found no significant difference in ONC201 efficacy when ONC201 was administered at a range of doses between 25 – 100 mg/kg via the oral and IP routes every 2 weeks (SFigure 2a). Moreover, weekly oral dosing of ONC201 appeared as effective as daily treatment (SFigure 2b, c). This suggests that the pharmacodynamic (PD) properties of ONC201 are maximal with weekly administration, and that weekly administration is more efficacious than less frequent dosing in mice. Importantly, administering a cumulative dose of 600 mg/kg of ONC201 given via six weekly 100 mg/kg doses did not cause toxicity or affect mouse weight or lower survival of the mice (SFigure 3a-c).

ONC201 triggers dual ERK/Akt inactivation, integrated stress response signaling (ISR), and TRAIL upregulation

We previously established that a single dose of ONC201 can lead to a blockade of Akt and ERK which is prolonged for up to 96 hours in vivo. Here we determined that there is no detectable effect on Akt/ERK or the ISR after 30 days following a single ONC201 dose. However, we found that the dual inhibition of Akt/ERK by ONC201 can still occur in a dose- and frequency-dependent manner in vivo; demonstrating the importance of dose-intensification on long term ONC201 pharmacodynamics in the clinic (Figure 2a). The degree of ISR activation as monitored by CHOP or ATF4 mRNA induction was significantly increased by administering

ONC201 more frequently (every 1-2 weeks versus every 3-4 weeks). On the other hand, increasing ONC201 dose did not further amplify CHOP upregulation at 50 or 100 mg/kg relative to 25 mg/kg given weekly (Figure 2b, SFigure 4a). We observed a frequency- but not a dose-dependent effect on serum TRAIL levels. Maximum serum TRAIL levels were achieved (150 pg/ml) when ONC201 was administered weekly even at low doses of 25 mg/kg (Figure 2c, SFigure 4b-c). Similar trends were observed with respect to overall TRAIL expression (SFigure 4d).

ONC201 inhibits metastasis, and migration and invasion, in a TRAIL-dependent mechanism

Given the potential anti-metastatic effects of TRAIL signaling, we hypothesized that ONC201 – as a compound that upregulates TRAIL and DR5 as part of its mechanism – would suppress metastatic tumor development. We observed that ONC201 reduces (in the case of the 25 mg/kg cohort) or inhibits metastases (in the case of higher dosed-cohorts) in these subcutaneous HT29 models (Figure 3a, S5a-c) and a secondary model where the subcutaneous primary tumor was surgically removed, and metastases allowed to grow before ONC201 treatment (Figure 3b). Increase in the ONC201 dose and administration frequency reduced the number, size, and incidence of metastases (SFigure 5a-c). In orthotopic MDA-MB-231 or subcutaneous HT29 xenograft-bearing mice, weekly MRI analysis and end-of-life bioluminescence imaging results confirmed that metastases develop independently of the primary tumor xenograft (Figure 3a, SFigure 5d-f). We observed a similar anti-metastasis effect of ONC201 in the immunocompetent subcutaneous CT26 xenograft model in syngeneic Balb/c mice and in HCT116-GFP mice that had their subcutaneous tumor removed at 10 mm diameter, with only the vehicle-treated mice showing metastatic cell populations (Figure 3b, SFigure 5g). This anti-metastasis effect was further observed using mice with HT29 or HCT116 $p53^{-/-}$ xenograft tumors on lungs from tail vein injected mice treated with vehicle or ONC201 after metastatic tumors were documented through CT imaging. Overall, the size of the metastases on the lungs decreased in the ONC201-treated cohorts while the vehicle-treated mice experienced growing tumors (Figure 3c-d, SFigure 5h). We also observed an impact on metastasis in mice treated with ONC201 or vehicle immediately after receiving tail vein injections (SFigure 5i).

ONC201 suppressed cell migration in vitro in HCT116 and HT29 cells as demonstrated by Boyden chamber and xCELLigence migration assays (SFigure 6a-d). TRAIL inhibition by the TRAIL-depleting RIK-2 antibody or shTRAIL attenuated the ONC201 effect on prevention of cell migration and invasion of MBA-MB-231 cells (Figure 4a, SFigure 6e). Invasion as assessed via a scratch assay was also impaired by ONC201, but was partially restored following treatment with RIK-2 (SFigure 6f). When investigated in vivo using the same tail vein method where mice were treated with ONC201 or vehicle once tumors were noted, we noticed a decrease in tumor size and number MDA-MB-231 wild-type bearing mice as compared to the MDA-MB-231 shTRAIL tumor-bearing mice (Figure 4b-c). This impact was also noted in mice treated immediately after tail vein injection of tumor cells (SFigure 5g-i). Interestingly, there was a slight difference observed in cleaved-caspase 3 levels between the tumor cohorts, but there was a statistically significant difference between the number of Ki67+ cells between the vehicle- and ONC201-treated mice bearing the wild-type tumors, and no significant difference in the mice bearing the shTRAIL tumors (Figure 4d-f). These results suggest that ONC201 inhibits metastasis, at least in part, by downregulating tumor cell migration and invasion in a TRAIL-dependent manner (17).

ONC201 induces CD3+/NK cell accumulation which plays an important role in the anti-tumor effect

Given the potential role of NK cells in preventing metastases through TRAIL that can be produced by NK cells (25), we investigated the presence of NK cells and other immune cells in ONC201-treated mice within the leukocyte population in colorectal MC38 and CT26 mouse tumors (SFigure 7-8). ONC201 induced an activation and accumulation of T and NK cells within tumors, blood, and spleen in two wild-type syngeneic mouse models and the NCR1-gfp mouse model (Bl6/129 background) (Figure 5a-c, SFigure 9a-d). Importantly, upregulation of NK+ and CD3+ cells was observed in blood of non-tumor bearing mice, indicating that the immune effect is not due to extrinsic signaling from ONC201-treated tumors alone (SFigure 9e). These ONC201-stimulated NK cells expressed granzyme at a higher MFI and expressed IFNγ (Figure 5d, SFigure 9f). Importantly, ONC201 activated

human primary NK cells from healthy donors by dramatically increasing IFNγ expression and causing increased de-granulation of the NK cells by increasing LAMP1 expression in the presence of target cells (Figure 6, SFigure 10). The recruitment of CD4+ and CD8+ cells to the tumor was also observed (SFigure 9g). The susceptibility of HCT116 *Bax*$^{-/-}$ and RKO-ONC201-resistant cells to ONC201 in vivo, despite their resistance to ONC201 in vitro, implicated involvement of an immune response in ONC201-mediated tumor suppression (Figure 7a, SFigure 11a). Importantly, depletion of NK cells with the anti-asialo GM1 antibody significantly attenuated the observed ONC201 anti-tumor efficacy in CT26, MC38, and *Bax*$^{-/-}$ tumor models despite there still being an increased presence of CD3+ T cells in the syngeneic models (Figure 7a-b, SFigure 11b-c). We found no significant impact from ONC201 on perforin-induced cytotoxicity on MC38 tumors by comparing ONC201 and vehicle treatments on MC38 tumor growth in both wild-type and perforin knockout (*Prf*$^{-/-}$) C57/BL6 mice (SFigure 11d-e). Interestingly, we saw no impact on T cell depletion using a CD8a inhibitor in MC38 mice in combination with ONC201, suggesting the role of NK cells may be more impactful on anti-tumor efficacy during ONC201 treatments than CD3+ cells (SFigure 11f-g).

To investigate the impact of ONC201's pro-immune response on metastasis, we analyzed metastases from tail vein injected HCT116, HCT116 *Bax*$^{-/-}$, and MC38 mice. We saw no increase in lymphocyte populations including NK cells or CD3+ cells in any of these metastases (SFigure 12).

ONC201's efficacy derives from direct tumor cell death and NK cell-related tumor cell death

Using the TRAIL-resistant HCT116 *Bax*$^{-/-}$ xenografts compared to wild-type HCT116 xenografts, we determined that ONC201's impact on *Bax*$^{-/-}$ tumor growth can be significantly attenuated when NK cells are depleted in vivo, whereas the effect of NK cell depletion on the sensitive wild-type cell line only slightly impacted anti-tumor efficacy (SFigure 13). However, there was still an anti-tumor effect from ONC201 treatment on HCT116 *Bax*$^{-/-}$ cells in NSG mice that carry no NK cells, T cells, or myeloid cells (SFigure 13c-d). We noted a slight decrease

in the number of Ki67+ cells when mice were treated with ONC201 and no change in cleaved caspase-3 (SFigure 13e-g).

PD-1 inhibitors in combination with ONC201 may enhance anti-tumor efficacy

We noted potent anti-tumor effects in vivo despite the presence of detectable increased PD-1 expression in CD3+ cells within ONC201-treated tumors, and given that ONC201 is efficacious in athymic nude mice we sought to leverage the ONC201-induced T cell effect in immunocompetent mice. We therefore explored the combination of ONC201 with anti-PD-1 therapy and preliminarily found evidence for more potent in vivo tumor suppression with the combination versus anti-PD-1 therapy alone (Figure 5e-f). This effect was not seen in low doses of ONC201 treatment of CT26-bearing mice or in MC38-bearing mice (SFigure 14a-g). Since we suspected the PD-1 expression may be present within T cells or NK cells (26, 27), we examined the impact of PD-1 on CD3+ cells in terms of ONC201 treatment using a combination of anti PD-1 and NK-depleting antibody anti-GM1. We saw only a slight but not significant difference in anti PD-1 treated cohorts when NK cells were depleted (SFigure 14f-g).

ONC201-induced NK activation/accumulation and anti-tumor effect is mediated through a pro-immune mechanism by upregulating several key factors including TRAIL, IFN-α2a and IP-10 (CXCL10)

We further investigated mechanisms by which NK cells contribute to ONC201 anti-tumor activity in vitro. To further explore the potential mechanism of ONC201-induced NK activation and accumulation, we performed a multiplex ELISA-based assay and identified immune-activating and recruiting factors that are upregulated in conditioned media of tumor cells in response to ONC201 treatment. This included IFNα-2a, IL-12p70, and the IFNγ-induced protein (IP-10 or CXCL10) (Figure 7e-f, SFigure 15). Cell culture experiments with NK92 cells confirmed in vivo results that ONC201 induces NK cell activation and TRAIL secretion (SFigure 16a-b). Complementing our in vivo data, co-culture studies of NK cells or conditioned media with tumor cells, including the ONC201-resistant HCT116 *Bax*$^{-/-}$ cells, confirms that the ONC201 anti-tumor effect occurs as a result of

ONC201 activation of NK cells since the inactive NK cells, or ONC201 treatment alone does not significantly induce tumor cytotoxicity in a model that is resistant to direct drug effects. (SFigure 13, 16c) Moreover, addition of TRAIL-sequestering antibody RIK2 reduced but did not eliminate the cytotoxic activity toward tumor cells. These results indicate that ONC201 efficacy is potentiated by ONC201 activation of NK cells to produce TRAIL (Figure 7c-d, SFigure 16c-d). Cell viability is further confirmed by a CTG assay and shows that ONC201-activated NK cells induce cytotoxicity at similar levels as observed with NK cells activated by IL-2 and IFNγ (SFigure 16e-f). Peripheral blood samples from patients who received ONC201 treatment showed an increase in the number of activated TRAIL-secreting NK cells after ONC201 treatment up to three days after treatment, further establishing that activated NK cells are upregulated by ONC201 treatment and express TRAIL (Table 1, Figure 8a-c).

Discussion

We demonstrate in this study that dose intensification of ONC201 increases anti-tumor drug efficacy, in part by amplifying ONC201's ability to induce TRAIL and activate the ISR, without impacting toxicity. In vivo, dose intensification sustains a more potent growth and survival pathway inhibition. The impact of these results is of immediate relevance to clinical trials where the frequency of administration is being increased to weekly dosing as a new recommended phase II dose (RP2D). We uncover a novel aspect of the anti-tumor effect of ONC201; namely, a powerful blockade of metastasis, that may be at least in part due to ONC201's ability to inhibit tumor cell migration and invasion. We unexpectedly discovered that ONC201 stimulates mobilization and activation of natural killer cell activity including infiltration of tumors in tumor-bearing mice, and cytotoxic effects of NK cells toward ONC201-sensitive or -resistant tumor cells. Optimum pharmacodynamic effects of ONC201 were observed with weekly dosing even though the drug half-life is 10 hours (9). Dose intensification of ONC201 increases the extent of the pro-survival kinase (Akt and ERK) inhibition leading to increased TRAIL expression and signaling in vivo, causing a more efficacious tumor growth inhibition and anti-metastasis effects. Given the impact of ONC201 on the number and size of colorectal xenograft metastases through both surgical model and tail vein injection, we can conclude that ONC201 suppresses metastases in vivo. While the role of TRAIL in ONC201's anti-metastasis effect is apparent in the in vitro studies; there was not a significant impact on TRAIL inhibition within the tumor in vivo. This may be due to the impact of TRAIL induction from ONC201 globally, and further studies suppressing TRAIL within the entire mouse may help clarify the importance of TRAIL in vivo. Further, we cannot rule-out other yet to be discovered mechanisms that may play a role in the ability of the drug to inhibit migration and invasion. Further studies are warranted to investigate other pathways activated by ONC201 that may play a role in the anti-metastasis effect. ONC201's ability to reduce migration is not dependent on its cytotoxic activity, and downregulation of the TRAIL pathway indicates that ONC201 exerts its anti-metastasis effects partially via a TRAIL-dependent mechanism [13]. Also, given that the strongest impact on

tumor growth within the MDA-MB-231 and shTRAIL tumors seemed to be from a decrease in Ki67+ cells, ONC201 may reduce metastasis by impeding other key events in tumor metastasis unrelated to TRAIL.

The increase, accumulation within tumors, and activation of NK cells both in vivo and in culture with human primary NK cells due to ONC201 treatment is unexpected and appears to promote tumor cytotoxicity in part through NK cell TRAIL secretion. As expected, the TRAIL-sequestering antibody did not completely abrogate NK cell-mediated cytotoxicity in cell co-culture, demonstrating that NK cells play a role in ONC201 efficacy that goes beyond TRAIL production. The significant cytotoxicity in the TRAIL-resistant *Bax*$^{-/-}$ cells in co-cultures with both NK cells and conditioned media indicate that NK cells promote cytotoxicity through its other tumor-suppression mechanisms namely cytokine secretion and direct NK-tumor cell contact (28). However, there was still efficacy in vivo, including within the *Bax*$^{-/-}$ carrying NSG mice. Given that there was a slight decrease in Ki67+ cells and there was an impact on tumor growth during ONC201 treatment regardless of immune-related cytotoxicity; it is likely that ONC201 may require both its intrinsic-direct cytotoxic mechanisms as well as a possible immune-response to suppress more ONC201-resistant tumors in vivo. Finally, although there appears to be an impact on degranulation in the human primary NK cells, interestingly there was no impact of ONC201 treatment in the perforin-/- mice compared to the wild-type mice. Since the MC38 tumors were still affected by ONC201 treatment, this may indicate the role of direct NK cell killing is not necessary for ONC201's pro-immune effects. Further studies of whether this could be mitigated in other tumors may clarify this further.

The immune effects of ONC201 play a role in the ONC201 mechanism of action in vivo that is highly relevant in ONC201-resistant tumors and contribute to anti-tumor effects in models where ONC201 sensitivity is observed in the absence of NK cells. We did not observe an increase in lymphocytes or immune cells in the larger metastases treated with ONC201. This could be due to the limited size of the metastases given that they were significantly smaller than our subcutaneous primary tumors. It is possible that given limitations of the size of metastases in mice that the role of immune stimulation with regard to the impact of ONC201 on metastases may be better

investigated in the context of the ONC201 clinical trials with human patients. Also, there could be an effect within the tumor microenvironment; as it is possible that ONC201's pro-immune response may not bypass a stroma-heavy tumor which may be a difference from subcutaneous tumors that are not surrounded by epithelium from the lung. Further, studies into the effect of ONC201 on the tumor microenvironment should be pursued to establish whether ONC201 can cause the tumor microenvironment to secrete anti-inflammatory cytokines and protect the tumor. Nonetheless, ONC201 has a potent anti-metastasis effect that is relevant to its use as cancer therapy in patients.

Importantly, our multiplex assay indicated that in response to ONC201 treatment, colorectal tumor cells secrete immune promoting factors. Of these, IFNα2-a, which induces sustained changes in NK cell responsiveness; IL-12p70, which enhances the cytotoxic activity of NK cells and induces differentiation and growth in T cells; and IP-10/CXCL10, a key chemo-attractant for T and NK cell recruitment; are all of interest and further establish that ONC201 has an immune-enhancing role. We plan to pursue further the mechanism of action of these extrinsic signaling pathways on NK cell activation as a result of ONC201 treatment. The induced cytotoxicity in co-culture is comparable to NK cell activation by increased IL-2 and IFNγ, without the added toxicity that these two cytokines provoke; making ONC201 a potentially attractive method of increasing the immune response (28, 29). The increase in CD3+ T cells shows a distinct promotion of the immune system with CD4+ and CD8+ T cells being present in the tumor. However, CD8a inhibition did not attenuate ONC201's efficacy, suggesting that the T-cells play less of an effect on ONC201's pro-immune effect. Further, the combination of anti-PD-1 therapy with ONC201 showed some increased efficacy in comparison to the anti-PD-1 monotherapy in CT26 tumors treated with high doses of ONC201; indicating that alleviating T cells of PD-1 expression may enhance ONC201's potency in vivo. However, we did not observe a clear advantageous impact of ONC201 and anti-PD-1 therapies in MC38 tumors or in CT26 tumors treated with lower ONC201 doses. This could be due to the inability of the TCR to recognize the tumors, given that the tumors are not MMR deficient and may not secrete enough clonal neo-epitopes. It is also possible that with lower ONC201 doses there may have been weaker signals for immune

stimulation. Further studies of whether there could be an advantage to ONC201 and anti-PD-1 therapies in combination may clarify these issues. Overall, the impact of ONC201 on immune-surveillance contributes to its efficacy in general and is particularly critical for promoting efficacy in some tumors that are resistant to ONC201 in vitro. There is probably sufficient preliminary evidence to support further testing of ONC201 plus anti-PD-1 in the clinic.

We demonstrate that higher or more frequent ONC201 dosing enhances the anti-tumor response, metastasis inhibition, and promotion of anti-tumor immunity. Dose intensification of ONC201 is now being explored in clinical trials to assess the proper regimen for different patient cohorts and is thus of immediate impact in the clinic. It is of clinical relevance that the pharmacodynamics (PD) effect of ONC201 extends for days to weeks beyond its serum half-life of 10 hours (9), and thus the most efficacious dosing in the clinic needs to be modeled by the PD characteristics. Additionally, we found no evidence that dosing based more on PK characteristics, i.e., daily dosing, provides any advantage over twice-weekly or weekly dosing. An important outcome of this study is the suggestion that, along with other biomarkers, monitoring of NK cell numbers, the state of NK cell activation in the blood and NK infiltration in post-treatment biopsies in patient tumors has potential to yield useful correlative clinical information with ONC201 efficacy. Initial patient data from a Phase II clinical trial demonstrates that patients who received ONC201 treatments exhibit increased NK cell populations in their peripheral blood. These NK cells were activated and secreted TRAIL, similar to what was observed in mice. The presence of these NK cells in tumor sites and in larger ONC201 treated patient populations will be further assessed. The activation of primary human NK cells by ONC201 may be considered for combination therapy in clinical trials using adoptive transfer of therapeutic NK cells. We note that unlike effects of PTEN (30) or the src inhibitor dasatinib (31), ONC201 inhibition of Akt and ERK pathways with consequent NK cell activation leads to potent anti-tumor cytotoxic effects in both co-culture experiments and in vivo. Moreover, unlike elotuzumab that can stimulate NK cell anti-tumor activity against multiple myeloma (32), ONC201 administration is not

associated with the well-known toxicities of IL-2 or TNF-α. The unique immune-stimulatory effect of ONC201 provides a rationale for combination therapy with complementary targeted therapeutics against cancer or checkpoint immunotherapy. With dose intensification, ONC201 has a higher likelihood for sustained TRAIL pathway activation in vivo, immune stimulation, and anti-metastasis effects.

Materials and Methods

Reagents and cell-based assays

All cell lines were obtained from the American Type Culture Collection or discussed previously. NK92 cells were provided by Kerry Campbell's lab at Fox Chase Cancer Center, Philadelphia PA. CT26 and MC38 cells were provided by Scott Waldman's lab at Thomas Jefferson University, Philadelphia PA. ONC201 was obtained from Oncoceutics, Philadelphia PA.

Western blot analysis and immunohistochemistry

Western blot analysis was conducted as previously described, with NuPAGE 4 to 12% bis-tris gel and visualized with ECL Prime Western Blotting Detection Reagent (Amersham) or SuperSignal West Femto (Thermo Scientific) and x-ray film and CytoSMART Live Imaging System (Lonza). For all cell lysis buffers, fresh protease inhibitor (Roche) was added immediately. All antibodies were purchased from Cell Signaling except anti-DR5 antibody (Abcam ab1675). After fixation, the tumor samples were embedded in paraffin and 8 μm sections were cut and mounted on slides. The sections were then processed and analyzed using immunohistochemistry with TRAIL, Ki67, Cleaved Caspase-3, CD3, and GFP antibodies similar to the method described previously (1). CD31, and Ki67 levels were calculated by independent blind-scoring and the use of VECTRA 3.0 Automated Quantitative Pathology Imaging system and Inform 2.0 software cursory of the Fox Chase Cancer Center Biosample Repository.

In vivo studies

All animal experiments were conducted in accordance with the Institutional Animal Care and Use Committee at Fox Chase Cancer Center. For subcutaneous xenografts, 6-week-old female athymic nu/nu mice (Taconic Biosciences) were inoculated with 1×10^6 cells of the HT29-luciferase, HCT116 *p53*$^{-/-}$, HCT116 *Bax*$^{-/-}$, RKO-ONC201-resistant, or HCT116-GFP cell lines in each rear flank, MDA-MB-231-luciferase in the lower mammary fat pads orthotopically, in a 150 μl suspension of 1:1 Matrigel (BD). For subcutaneous xenografts in syngeneic models, CT26 cells were inoculated with 1.0×10^6 cells into six-week old female Balb/c mice (Taconic

Biosciences) and MC38 cells were inoculated with 1.0 x 10^6 cells into six-week old female C57/BL6 mice (Taconic Biosciences), six-week old female BL6/129-NCR1-GFP mice (Jackson Laboratories), or six-week old female C57BL/6-*Prf1*^{tm1Sdz}/J (Jackson Labs). All subcutaneous tumors were allowed to establish for 1 to 3 weeks after injection until they reached a volume of ~150-200 mm^3 before treatment initiation. Mice were monitored every 3 days and tumors volumes were measured using calipers. For the surgical method, mice were anesthetized using isoflurane after the tumors reached 1000 mm^3, and the tumor was removed by making an incision around the skin and carefully scraping out the tumor. All bleeding was controlled, and the wound closed using surgical wound clips. Mice were monitored every 6 hours for 2 days until they recovered. For tail vein injections, the same cell number used above for each tumor type was placed into 150 μl and injected through the tail vein. Mice were monitored daily for the first 3 days.

ONC201 injections were administered subcutaneously at indicated doses in 20:80 DMSO:PBS or orally in 10:70:20 DMSO:PBS:Cremphor El as described [1]. GM1 was delivered every 5 days (Wako, 986-10001). PD-1 was injected 200 μg every 3 days (Bio Xcell BE1046). CD8-a inhibitor was injected at 400 μg twice a week (Bio Xcell 0061). PD-1 inhibition and staining was confirmed by staining one ONC201 monotherapy treated tumor with either the Bio XCell PD-1, PD-1 PE from ebioscience, or Bio XCell PD-1 for 2 hours then staining with PD-1 PE. The resulting staining indicated that the Bio XCell PD-1 is a true inhibitor of PD-1 (SFigure 14f). Tumor volumes were measured according to the formula (L*W^2)/2.

In vivo pathology and toxicology

Toxicity during the course of ONC201 treatment was adjudged by body weight decrease of greater than 10%, tumor growth of more than 10% of body weight, or a body condition scoring <2. Serum and plasma samples were collected through orbital bleeding and cardiac puncture before sacrifice, and were immediately stored at 4^{o}C and processed by Antech Diagnostics for CBC and chemistry panels. Results were analyzed by board-certified toxicologists. Tumors were measured post-mortem through caliper and water density examination. Organ and

tumor samples were processed in 10% formalin and fixed in paraffin. Hematoxylin-stained samples were analyzed by a board-certified pathologist to determine whether tumor cells existed on any organs or necrosis occurred in tumors. Board-certified veterinary pathologists also indicated whether or not signs of toxicity were present.

In vivo mouse tumor imaging

For luciferase cell lines, D-Luciferin from Gold Bio was administered weekly following manufacturers' instructions (60 μL, 50 mg/ml stock) and imaging was performed on a Xenogen IVIS system (Xenogen, Almadea, CA). MRI imaging was performed in a vertical-bore 7-T magnet with a Bruker DRX300 spectrometer (Bruker Biospin Corporation, Billerica, MA) and ParaVision 3.0 software (Bruker Biospin Corporation) through the Fox Chase Imaging Core Facility. Custom-built transfer cassette constructed to compress the mice to an equal thickness of 15.0 mm as described were used within the MRI to keep the mouse still and administer isoflurane gas. GFP imaging was performed using the Maestro in vivo imaging system (Cri, Woburn, MA) and the Nuance multi-spectral imaging system (Cri, Cambridge, MA). Image data sets were converted and tumor volumes were calculated using Para Vision. Final images were converted to ImageJ format. For CT imaging, all mice were imaged in a Sofie Biosciences G8 scanner (Sofie Biosciences, Culver City, CA) under isoflurane. CT data sets were acquired with an isotropic voxel size of 200 microns^3. Mice were maintained under isoflurane anesthesia for the duration of the scan. For analysis, the thoracic cavity was segmented into compartments comprising the heart, lung airspace, lung tissue, and discrete tumors on the CT data sets. The lung airspace was segmented on the CT scans with a connected nearest neighbor seed growing algorithm, using one voxel in the lung as a seed point, and manually setting the seed thresholds. The lung tissue present outside the airspace, as well as any structures identified as tumors, were determined manually using a 3D region of interest tool. All image analyses were performed with Vivoquant software (Invicro Inc.; Boston, MA)

ELISA assays

A total of 100-150 μL blood was collected through orbital blood draw as described above and plasma was collected in EDTA tubes and serum collected in Heparin separating tubes. Tubes were spun at 1,000 rpm for 15

min. Samples were analyzed using Human TRAIL/TNSFSF10 Quantikine ELISA kit (R&D Systems, Minneapolis MN). All analyses were performed under manufacturer's directions.

For conditioned media studies, a mesoscale multiplex ELIS assay was used. Conditioned media was harvested from the cell lines at designated times and doses. Three separate conditioned media samples per cohort where harvested and ran in duplicate. The mean of each duplicate was taken and compared using a 2-sided Wilcoxon rank sum test

In vitro tumor migration and invasion assays

Boyden assays were performed using the QCM ECMatrix Cell invasion assay (Millipore, ECM550) and the cultrex cell migration assays (R&D systems, 3465-096-K). Cell migration and invasion were also assessed using the real-time xCelligence system. Invasion assays in the xCelligence system were conducted with Matrigel (33). Wound healing assays were performed with the CytoSelect Wound healing assay kit (Cell BioLabs, CBA-120T). Cell viability was confirmed by tryphan blue or Cell TiterGlo, data was only included if cell viability was above 75%.

In vitro tumor and natural killer NK cell co-culture

NK92 cells were maintained in 4% IL-2 media and before experiment were maintained in low IL-2 (1%) containing media. Tumor cell lines were plated at 30,000 cells/well in an 8-well chamber slide for 24 hours. NK92 cells were washed, suspended in fresh media, and then plated over the tumor cells at a concentration of 80,000 cells/mL. Alternatively, the conditioned media (media as shown in Figures) from the NK cells cultured for 48 hours was added to the tumor cells. After 48 hours of co-culturing, NK92 cells were removed and both NK cells and tumor cells were stained with calcein blue and ethidium homodimer. Non-GFP expressing tumor cells were labeled with anti-EPCAM-1 antibody (1:200) followed by the Alexa-488 secondary (1:200). NK92 cells were labeled with CD56-APC (Biolegend, 318309). Immunofluorescence was performed on the Nuance Multi-spectral imaging system (Cri, Cambridge, MA). As an alternative for measuring tumor cell viability in co-culture, the CellTiter-Glo assay (Promega, Madison, WI as directed) was used directly after NK cells were removed. Plates

were analyzed using the IVIS described in animal methods. As controls, NK92 cells were incubated in high IL-2 (4%) containing media 400 units/mL IFNγ.

In vitro primary NK cell analysis

Primary NK cells were acquired from peripheral blood of healthy donors per IRB protocol. Lymphocytes were isolated through lymphoprep (Stem Cell 07801) centrifugation and NK cells were isolated using the EasySep Human NK cell isolation kit and magnet per manufactures instructions (Stem Cell 17955). NK cells were then incubated overnight with 1% IL-2 +/- ONC201. IFNγ assay was performed by incubating cells with IFNγ and then incubated with IFNγ-PE and antibodies listed in SFigure 10a. LAMP1+ assay was performed by incubating NK cells alone, with 721.221 target cells, or target cells and 100 ng/ml of rituxumab. NK cells only degranulate in the presence of 721.221 target cells, allowing us to measure LAMP1+ expression of activated NK cells, and rituximab was used as the positive control which increases de-granulation. Cohorts were as described: PBL, PBL ONC: NK cells alone or with ONC201; PBL+721.221, PBL + 721 ONC: NK cells incubated with target cells +/- ONC201; PBL+721+Rxb, PBL+721.221+Rxb ONC: NK cells incubated with target cells and rituximab +/- ONC201. Cells were then rinsed and stained with LAMP 1+ and antibodies listed in SFigure 10b. Gating strategies can be seen in SFigure 10.

Flow cytometry

For flow cytometry analyses, antibodies were purchased from eBioscience unless otherwise indicated. Analysis was performed by incubating cells for 30 minutes on ice with 20 μg/ml purified Fab antibody. Cells were stained with 1% FBS, 0.09% Sodium Azide in PBS and red blood cells were lysed in red blood lysis buffer (155 mM NH_4Cl, 12 mM $NaHCO_3$, 0.1 mM EDTA in PBS). Cells were then washed and incubated in 2 μg/mL propidium iodide (PI) in staining buffer. Analyses were performed as seen SFigure 7-8. Cellular concentrations of select antibodies were determined with LSRII (Beckton Dickinson, San Jose, CA) and analyzed with FlowJo software (Tree Star, San Carlos, CA).

Patient Analysis

Cells from patients treated with ONC201 (NCT02250781) were obtained by peripheral blood draw. Peripheral blood mononuclear cells were isolated from blood on the day of the blood draw by Ficoll-Hypaque density centrifugation and frozen prior to analysis in CryoStor solution (BioLife Solutions, Bothell, WA). Thawed cells were washed in PBS and incubated with fluorescent-labeled antibodies at 4^{o}C for 20 minutes for extracellular staining, permeabilized, and incubated with fluorescent-labeled antibodies at 4^{o}C for 30 minutes for intracellular staining. Analysis of live, non-debris, singlet, leukocytes was performed as previously described in (34) using an LSRII flow cytometer (Beckton Dickinson) and with FlowJo software (Tree Star).

Steps to maintain optimum viability of cryopreserved cells for future analyses were taken. Processing of patient blood samples occurred within one hour of blood draw and slow freezing of cells was performed immediately after processing to increase viability. Cryopreserving these cells in this way and then thawing them all at the same time (and antibody staining and flowing them at the same time) ensures similar testing and analyses on all samples and increases the accuracy of the results. Further, all cells were cryopreserved in Cryostor CS10, a solution that mitigates temperature-induced molecular cell stress responses during freezing and thawing. As described by the manufacturer (and observed in our laboratory compared to 90% FBS/10%DMSO), this solution has been proven much more effective in reducing post-preservation necrosis and apoptosis compared to commercial and home-made formulations. Citations of cell preservation capabilities and comparisons to other solutions are available from the manufacturer (BioLife Solutions). Importantly, after thawing, viability analysis demonstrated >80% live CD45+ cells across all samples, demonstrating the efficacy of our cryopreservation process and ensuring that analysis produced accurate results. As expected, the immune cell populations among PBMCs varied across the 5 patients and across the 3 time points collected for each patient (as seen in Figure 8 where the NK cells varied across patients and over the 3 time points for each patient). However, overall, populations across the sum of samples analyzed were found to be at proportions that are still within the normal variation and range for patient samples, including T cells (53% [expected 45-70% of PBMCs]), B cells (5% [expected 3-15%]), NK cells (8% [expected 5-20%]), Monocytes (26% [expected [15-35%]]. In patients where the CD3-CD19- (non-T/non-B)

population was increased (as in patient 1), the majority population was monocytes. This would not be an expected artifact of the cryopreservation process as the myeloid lineage cells are more likely to be lost in cryopreservation than lymphocytes, yet here the proportions of monocytes are increased at a few individual time points. Cell proportions normalized with ONC201 treatment and as in mouse model studies, NK cell proportions and function were augmented.

Statistical analysis

Data are presented as means + SD. To assess the statistical significance of the differences between group comparisons (Vehicle vs ONC201, ONC201 vs ONC201 + PD-1), of tumor volume before and after treatment in the tail vein, xenograft, RLU, blood serum, gene expression, and protein expression experiments, 2-side Wilcoxon rank sum test was used. For in vitro, measurements from three biological replicates per treatment group were compared unless noted in the Figure legends. When there were more than 2 observations made xenograft study: the means per mouse (for example, 3 IHC slides were analyzed per tumor, the mean of each tumor) were compared using a 2-sided Wilcoxon rank sum test. For supplemental figure 6g, metastases were grouped '<2' and '$\geq$2' for the comparison between wildtype and shTRAIL ONC201 groups using 2-sided Fisher's exact test. For patient samples in Figure 8, statistical significance was determined by a paired 2-sided t-test. For all tests, $P < 0.05$ was deemed statistically significant. Unless otherwise noted in the Figure legends, comparisons were made against the vehicle control.

Study Approval

For animal studies, all animals were housed and handled in accordance with the Institutional Animal Care and Use Committee of Fox Chase Cancer Center, Philadelphia PA. All studies were performed in accordance with national animal protection laws.

For patient studies at Rutgers, the IRB used to obtain patient samples was: IRB protocol #Pro20140000405 titled "A phase I single-agent open-label dose-escalation study of oral ONC201 in patients with advanced solid

tumors". The protocol approval was obtained from Health Sciences IRB - New Brunswick/Piscataway 335 George Street Suite 3100, 3rd Floor New Brunswick, NJ 08901 and was initially approved 10/3/14. The latest version of this protocol was approved 12/20/2017 and expires 06/05/2018. All patients signed informed consent for trial participation.

For healthy human NK study the IRB is FCCC #99-802, and was last renewed on 5/18/17, expiring 5/17/18.

Author contributions

J.W. and W.S.E-D. designed all the experiments. J.W. conducted the experiments and wrote the manuscript. C.L.K. assisted in all animal experiments and qRT-PCR work. L.Z. assisted in all imaging including IHC and co-culture experiments. K.C. and A.M. assisted in the design and experimental procedures of human primary NK cell work. K.Q.C. assisted with all pathological analysis and IHC analysis. H.H.H. assisted with mouse CT imaging. C.B.C. and J.H.N. conducted NK cell studies utilizing patient-derived samples from ONC201 clinical trial, and A.Z. analyzed the patient data and wrote the related manuscript sections. A.J.O. contributed to the conceptualization and rationale of the dose intensification experiments. E.R. contributed to the appropriate analytical methods. This work was presented in part at the 2016 American Association for Cancer Research (AACR) meeting in New Orleans, LA, the 2016 American Society for Clinical Oncology (ASCO) meeting in Chicago, IL, and in the 2017 AACR meeting in Washington D.C. J.W. received the 2016 AACR-Triple Negative Breast Cancer Foundation training award for this work. W.S.E-D. conceptualized and supervised the experiments and contributed as senior author including editing of the manuscript and responsibility for oversight of conduct of the research.

Competing interests: W.S.E-D. is a co-founder of Oncoceutics Inc., and is fully compliant with institutional and NIH disclosure guidelines.

Acknowledgements

We thank the Fox Chase Cancer Center Animal Facility and Small Animal Imaging Component of the Biological Imaging Facility at FCCC, and support from the National Cancer Institute (Grant Number CA-006927) for assistance in animal imaging. We want to thank the Animal Histopatholgy Facility and Biosample Repository at the Fox Chase Cancer Center for assistance with pathology and IHC analysis. We also thank Anthony Lerro and the Fox Chase Cancer Center Animal Facility for assistance with the surgeries and tail vein injections. W.S.E-D. is an American Cancer Society Research Professor. **Funding:** This work was supported by grants from the NIH

(CA173453 to W.S.E-D.), the American Cancer Society (to W.S.E-D.), and the William Wikoff Smith Endowed Professorship in Cancer Research (to W.S.E-D.).

References

1. Allen JE, Krigsfeld G, Mayes PA, Patel L, Dicker DT, Patel AS, et al. Dual inactivation of Akt and ERK by TIC10 signals Foxo3a nuclear translocation, TRAIL gene induction, and potent antitumor effects. *Sci Transl Med.* 2013;5(171):171ra17.
2. Allen JE, Krigsfeld G, Patel L, Mayes PA, Dicker DT, Wu GS, et al. Identification of TRAIL-inducing compounds highlights small molecule ONC201/TIC10 as a unique anti-cancer agent that activates the TRAIL pathway. *Mol Cancer.* 2015;14(1):99.
3. Allen J, Kline C, Prabhu V, Wagner J, Ishizawa J, Madhukar N, et al.: Oncotarget; 2016.
4. Ishizawa J, Kojima K, Chachad D, Ruvolo P, Ruvolo V, Jacamo RO, et al. ATF4 induction through an atypical integrated stress response to ONC201 triggers p53-independent apoptosis in hematological malignancies. *Sci Signal.* 2016;9(415):ra17.
5. Kline CL, Van den Heuvel AP, Allen JE, Prabhu VV, Dicker DT, and El-Deiry WS. ONC201 kills solid tumor cells by triggering an integrated stress response dependent on ATF4 activation by specific eIF2α kinases. *Sci Signal.* 2016;9(415):ra18.
6. Allen JE, Crowder RN, Crowder R, and El-Deiry WS. First-In-Class Small Molecule ONC201 Induces DR5 and Cell Death in Tumor but Not Normal Cells to Provide a Wide Therapeutic Index as an Anti-Cancer Agent. *PLoS One.* 2015;10(11):e0143082.
7. Prabhu VV, Allen JE, Dicker DT, and El-Deiry WS. Small-Molecule ONC201/TIC10 Targets Chemotherapy-Resistant Colorectal Cancer Stem-like Cells in an Akt/Foxo3a/TRAIL-Dependent Manner. *Cancer Res.* 2015;75(7):1423-32.
8. Allen JE, Prabhu VV, Talekar M, van den Heuvel AP, Lim B, Dicker DT, et al. Genetic and Pharmacological Screens Converge in Identifying FLIP, BCL2, and IAP Proteins as Key Regulators of Sensitivity to the TRAIL-Inducing Anticancer Agent ONC201/TIC10. *Cancer Res.* 2015;75(8):1668-74.
9. Allen JE, Kline CL, Prabhu VV, Wagner J, Ishizawa J, Madhukar N, et al. Discovery and clinical introduction of first-in-class imipridone ONC201. *Oncotarget.* 2016.
10. Wagner J, Kline CL, Pottorf RS, Nallaganchu BR, Olson GL, Dicker DT, et al. The angular structure of ONC201, a TRAIL pathway-inducing compound, determines its potent anti-cancer activity. *Oncotarget.* 2014;5(24):12728-37.
11. Jin ZZ, Wang W, Fang DL, and Jin YJ. mTOR inhibition sensitizes ONC201-induced anti-colorectal cancer cell activity. *Biochem Biophys Res Commun.* 2016;doi: 10.1016/j.bbrc.2016.08.126. .
12. Zhang Q, Wang H, Ran L, Zhang Z, and Jiang R. The preclinical evaluation of TIC10/ONC201 as an anti-pancreatic cancer agent. *Biochem Biophys Res Commun.* 2016;476(4):260-6.
13. Stein MN, Bertino JR, Kaufman HL, Mayer T, Moss R, Silk A, et al. First-in-human Clinical Trial of Oral ONC201 in Patients with Refractory Solid Tumors. *Clin Cancer Res.* 2017.
14. J W, CL K, and W E-D. *ASCO*. Chicago IL; 2016.
15. Elrod HA, Fan S, Muller S, Chen GZ, Pan L, Tighiouart M, et al. Analysis of death receptor 5 and caspase-8 expression in primary and metastatic head and neck squamous cell carcinoma and their prognostic impact. *PLoS One.* 2010;5(8):e12178.
16. Grosse-Wilde A, Voloshanenko O, Bailey SL, Longton GM, Schaefer U, Csernok AI, et al. TRAIL-R deficiency in mice enhances lymph node metastasis without affecting primary tumor development. *J Clin Invest.* 2008;118(1):100-10.
17. Takeda K, Hayakawa Y, Smyth MJ, Kayagaki N, Yamaguchi N, Kakuta S, et al. Involvement of tumor necrosis factor-related apoptosis-inducing ligand in surveillance of tumor metastasis by liver natural killer cells. *Nat Med.* 2001;7(1):94-100.
18. Cretney E, Takeda K, Yagita H, Glaccum M, Peschon JJ, and Smyth MJ. Increased susceptibility to tumor initiation and metastasis in TNF-related apoptosis-inducing ligand-deficient mice. *J Immunol.* 2002;168(3):1356-61.
19. Shin MS, Kim HS, Lee SH, Park WS, Kim SY, Park JY, et al. Mutations of tumor necrosis factor-related apoptosis-inducing ligand receptor 1 (TRAIL-R1) and receptor 2 (TRAIL-R2) genes in metastatic breast cancers. *Cancer Res.* 2001;61(13):4942-6.

20. Zhuang L, Lee CS, Scolyer RA, McCarthy SW, Zhang XD, Thompson JF, et al. Progression in melanoma is associated with decreased expression of death receptors for tumor necrosis factor-related apoptosis-inducing ligand. *Hum Pathol.* 2006;37(10):1286-94.
21. Levy EM, Roberti MP, and Mordoh J. Natural killer cells in human cancer: from biological functions to clinical applications. *J Biomed Biotechnol.* 2011;2011:676198.
22. Gross E, Sunwoo JB, and Bui JD. Cancer immunosurveillance and immunoediting by natural killer cells. *Cancer J.* 2013;19(6):483-9.
23. Sun JC, and Lanier LL. NK cell development, homeostasis and function: parallels with $CD8^+$ T cells. *Nat Rev Immunol.* 2011;11(10):645-57.
24. Stein M, Mayer T, Moss R, Silk A, Chan N, Haffty B, et al. *2015 ASCO Annual Meeting*. Chicago, IL: http://meetinglibrary.asco.org/content/166310-176; 2016.
25. Smyth MJ, Cretney E, Takeda K, Wiltrout RH, Sedger LM, Kayagaki N, et al. Tumor necrosis factor-related apoptosis-inducing ligand (TRAIL) contributes to interferon gamma-dependent natural killer cell protection from tumor metastasis. *J Exp Med.* 2001;193(6):661-70.
26. Concha-Benavente F, Srivastava R, Kansv B, and Ferris R. PD-1 is a marker of activation on tumor infiltrating NK cells in head and neck cancer. *J Immunother Cancer* 2015;3:398.
27. Wei F, Zhong S, Ma Z, Kong H, Medvec A, Ahmed R, et al. Strength of PD-1 signaling differentially affects T-cell effector functions. *Proc Natl Acad Sci U S A.* 2013;110(27):E2480-9.
28. Zamai L, Ponti C, Mirandola P, Gobbi G, Papa S, Galeotti L, et al. NK cells and cancer. *J Immunol.* 2007;178(7):4011-6.
29. Jonasch E, and Haluska FG. Interferon in oncological practice: review of interferon biology, clinical applications, and toxicities. *Oncologist.* 2001;6(1):34-55.
30. Briercheck EL, Trotta R, Chen L, Hartlage AS, Cole JP, Cole TD, et al. PTEN is a negative regulator of NK cell cytolytic function. *J Immunol.* 2015;194(4):1832-40.
31. Hassold N, Seystahl K, Kempf K, Urlaub D, Zekl M, Einsele H, et al. Enhancement of natural killer cell effector functions against selected lymphoma and leukemia cell lines by dasatinib. *Int J Cancer.* 2012;131(6):E916-27.
32. Balasa B, Yun R, Belmar NA, Fox M, Chao DT, Robbins MD, et al. Elotuzumab enhances natural killer cell activation and myeloma cell killing through interleukin-2 and TNF-α pathways. *Cancer Immunol Immunother.* 2015;64(1):61-73.
33. Eisenberg MC, Kim Y, Li R, Ackerman WE, Kniss DA, and Friedman A. Mechanistic modeling of the effects of myoferlin on tumor cell invasion. *Proc Natl Acad Sci U S A.* 2011;108(50):20078-83.
34. Zloza A, Kohlhapp FJ, Lyons GE, Schenkel JM, Moore TV, Lacek AT, et al. NKG2D signaling on $CD8^+$ T cells represses T-bet and rescues CD4-unhelped $CD8^+$ T cell memory recall but not effector responses. *Nat Med.* 2012;18(3):422-8.

Table 1: Characteristics of patients 1-5 (P1-P5)

treated with ONC201.

Patient	Tumor type	Age	Sex
P1	Prostate	70	M
P2	Prostate	61	M
P3	Prostate	64	M
P4	Prostate	78	M
P5	Prostate	73	M

A

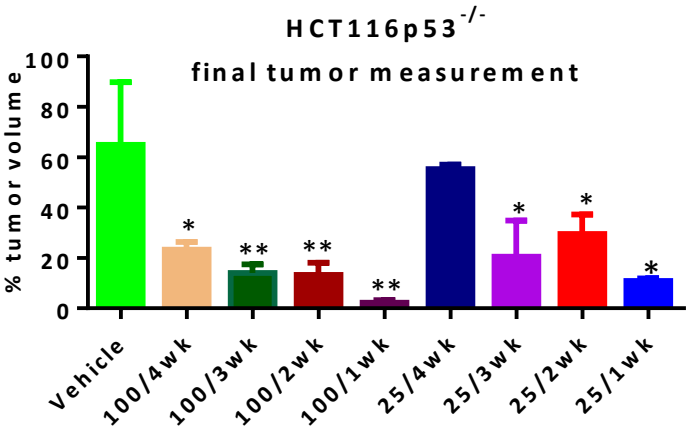

B

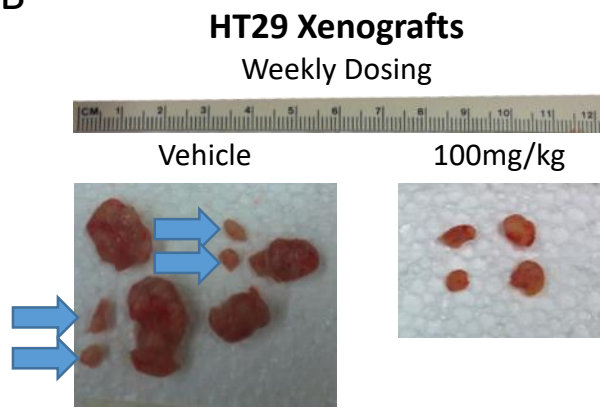

C

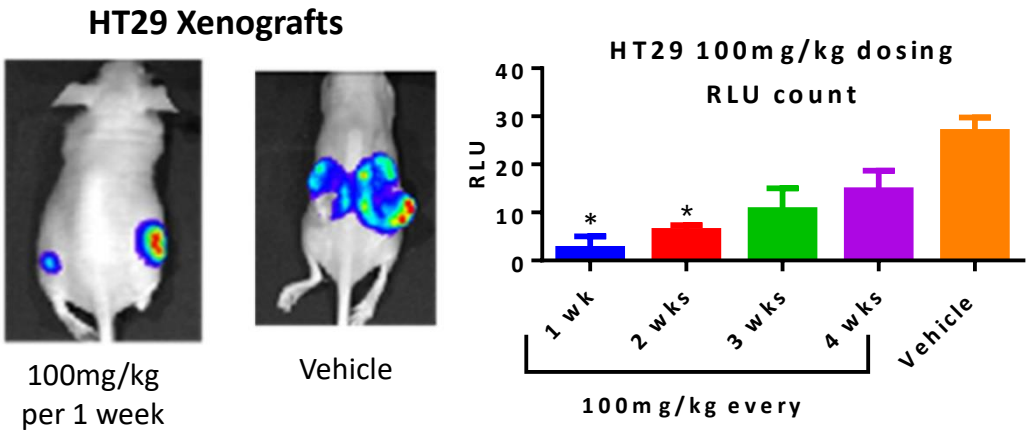

Wagner *et al.*, Figure 1

Figure 1. ONC201 dose intensification negatively impacts tumor growth and metastasis. (A) Mouse cohorts received 25 mg/kg or 100 mg/kg weekly, every 2, 3, or 4 wks. Shown is the percent tumor growth of both dose and frequency of ONC201 over time in the athymic female nude mice using HCT116 *p53*$^{-/-}$ colorectal cancer xenografts (B) Final HT29-luc tumors of cohorts administered 100 mg/kg or vehicle treatment ONC201 weekly harvested after 4 wks. Blue arrows indicate metastatic tumors. (C) Final HT29-luc bioluminescence of cohorts administered with 100 mg/kg at different frequencies and harvested after 4 weeks with corresponding RLU from whole cohort. N=6 in HT29 and HCT116 *p53*$^{-/-}$. Percent tumor calculated by diving each tumor volume by the average tumor volume of the vehicle and multiplying by 100. (P values are as indicated: * < 0.05, ** < 0.01 compared to the vehicle unless indicated using 2-side Wilcoxon rank sum test). Data represent mean +/- SD.

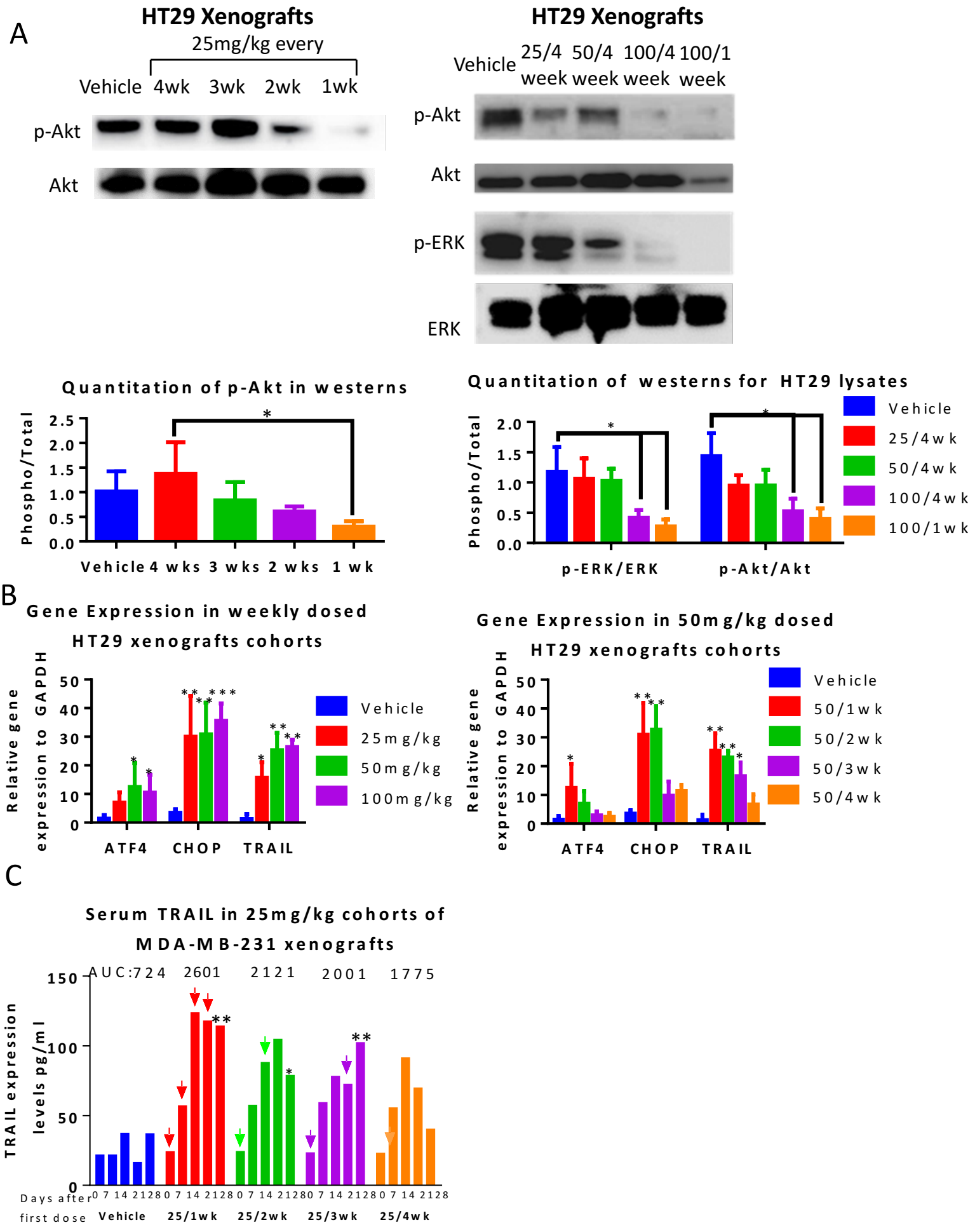

Wagner *et al.*, Figure 2

Figure 2. ONC201 triggers dual ERK/Akt inactivation, integrated stress response (ISR) signaling, and TRAIL upregulation in tumor cells. (A) HT29 tumor xenograft protein lysates analyzed by western blots treated with (left) 25 mg/kg at varying frequencies and (right) increasing dose up to 100 mg/kg and varying frequency of administration as indicated. (B) Induction of ATF4, CHOP, and TRAIL mRNA in HT-29 xenografted tumors following (left) increasing dose with weekly administration of ONC201 or (right) frequency of ONC201 dosing at 50 mg/kg. (C) Serum TRAIL levels measured by non-specific ELISA comparing following ONC201 25 mg/kg dose administered at different frequencies in MDA-MB-231 xenograft bearing mice. Doses indicated by arrows. AUC values listed above and graphed to the right. (For western blots and qRTPCR: N=6, ran twice in triplicate of each sample. For ELISA, n=4 ran in duplicate, samples were frozen until end of assay and ran through ELISA) (All samples were harvested 4 weeks after treatment began unless indicated). (P values are as indicated: * < 0.05, ** < 0.01 compared to the vehicle unless indicated 2-side Wilcoxon rank sum test, for c, only the last time-point was analyzed for statistical significance). Data represent the mean +/- SD.

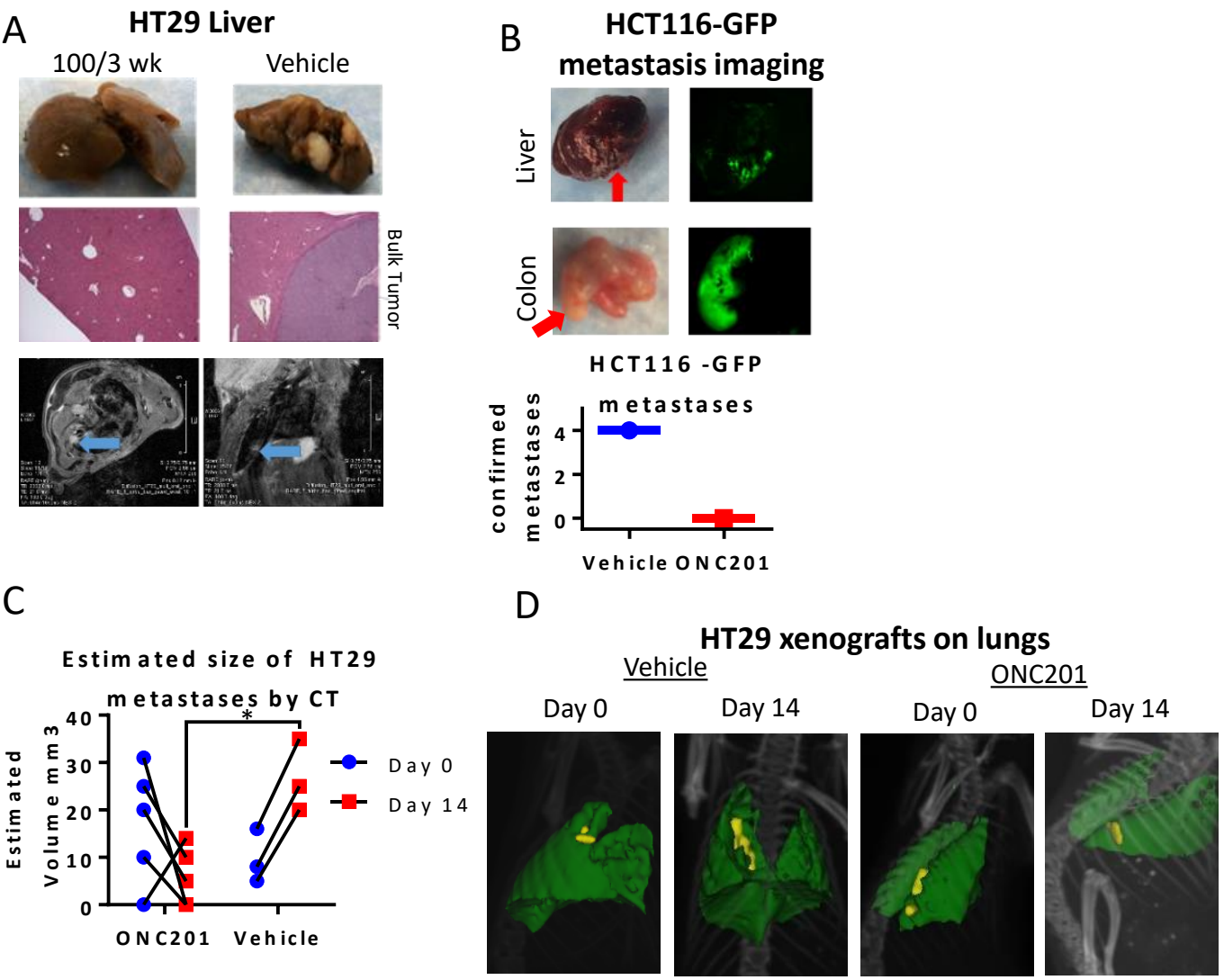

Wagner *et al.*, Figure 3

Figure 3. ONC201 inhibits metastasis in vivo. (A) Metastasis imaging analyzed by (top) gross and histology of liver in HT29 xenograft bearing mice treated with vehicle or 100 mg/kg per 3 wks. (bottom) MRI of lung of HT29 subcutaneous xenograft mouse treated with vehicle after 4 weeks since inoculation. Both panels are imaging of 1 vehicle mouse from different MRI viewpoints. The tumor is indicated by a blue arrow. (B) HCT116-GFP tumor lesions from mice with primary tumor surgically removed and tumor metastases allowed to grow overtime before treatment. Identified by fluorescence imaging for vehicle or 100 mg/kg ONC201. (C) Estimated size by CT imaging before and after treatment in ONC201 and Vehicle treated cohorts in HT29 xenografts. (D) representative CT images of HT29 treated mice through tail vein injection. Tumor burden in yellow, lung tissue in green. Same mouse Day 0 and Day 14. (For mouse tumor studies, mouse numbers N=6 in HT29 subcutaneous in a and tail-vein HT29 in c and d, N=4 HCT116 GPF. In C, 2 vehicles passed away before end of study. All samples were harvested 4 weeks after treatment began unless indicated). (P values are as indicated: * < 0.05 compared to the vehicle unless indicated 2-side Wilcoxon rank sum test, with difference between post/pre-treatment compared). Data represent the mean +/- SD.

A

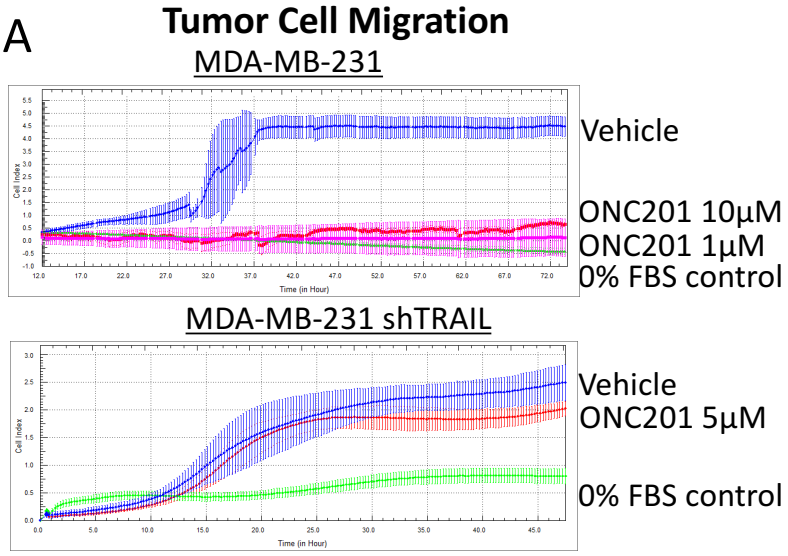

B

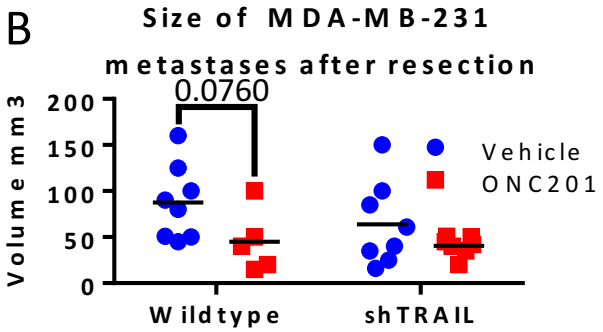

C

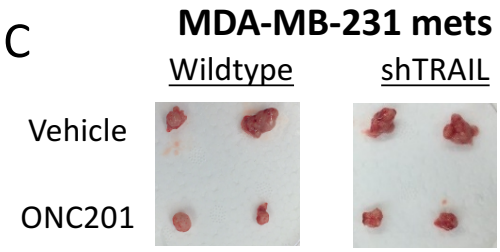

D

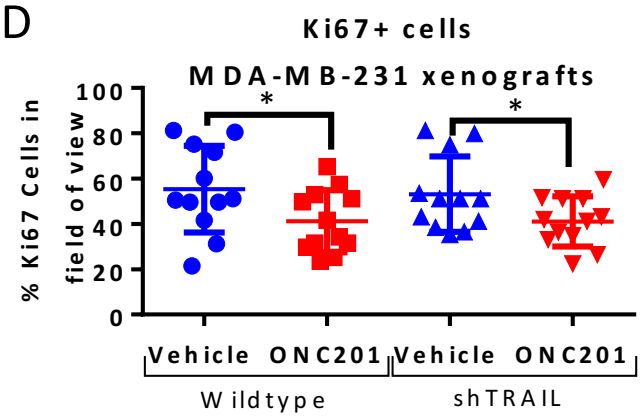

E

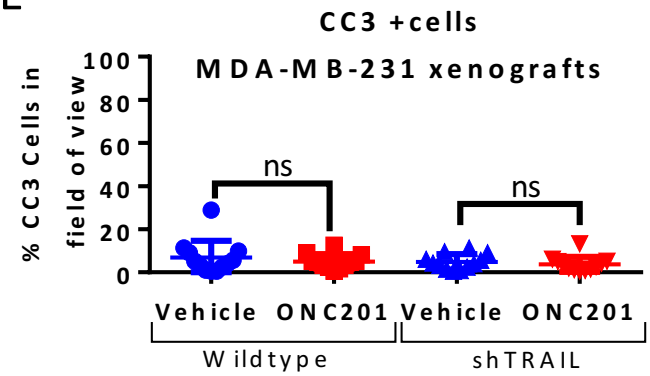

F

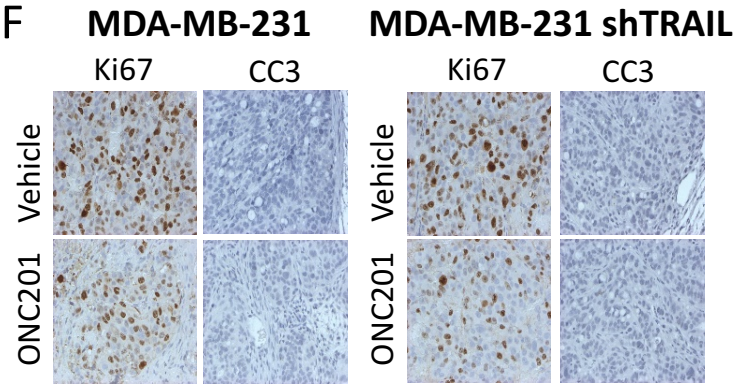

Wagner *et al.*, Figure 4

Figure 4. ONC201 inhibits migration/invasion and metastasis in partially TRAIL-dependent manner. (A) Xcelligence migration kinetics assay in top) MDA-MB-231 and bottom) MDA-MB-231 shTRAIL. (B) Size of MDA-MB-231 wildtype and shTRAIL tumors from tail vein injected mice after treatment for two weeks and then resection. Mice were treated once tumor burden noted (tumor burden tended to line on the spinal cord). (C) Representative image of MDA-MB-231 wildtype and shTRAIL tumors after resection. (D) Quantification of Ki67+ cells in MDA-MB-231 wildtype and shTRAIL xenografts of ONC201 and Vehicle cohorts. N=12 slides, 3 per tumor. (E) Quantification of cleaved caspase-3 positive cells in MDA-MB-231 wildtype and shTRAIL xenografts of ONC201 and Vehicle cohorts. N=12 slides, 3 per tumor. N=12 slides, 3 per tumor. (F) Representative images of both using 20x magnification. (For mouse tumor studies, N=5 for MDA-MB-231 and MDA-MB231 shTRAIL. For in vitro migration/invasion studies, N=4 ran two separate times. All samples were harvested 4 weeks after treatment began unless indicated). (P values are as indicated: * < 0.05, ** < 0.01 compared to the vehicle unless indicated using 2-sided Wilcoxon rank sum test. For IHC studies when 3 IHC slides were analyzed per tumor, the mean of each tumor was compared using a 2-sided Wilcoxon rank sum test). Data represent the mean +/- SD.

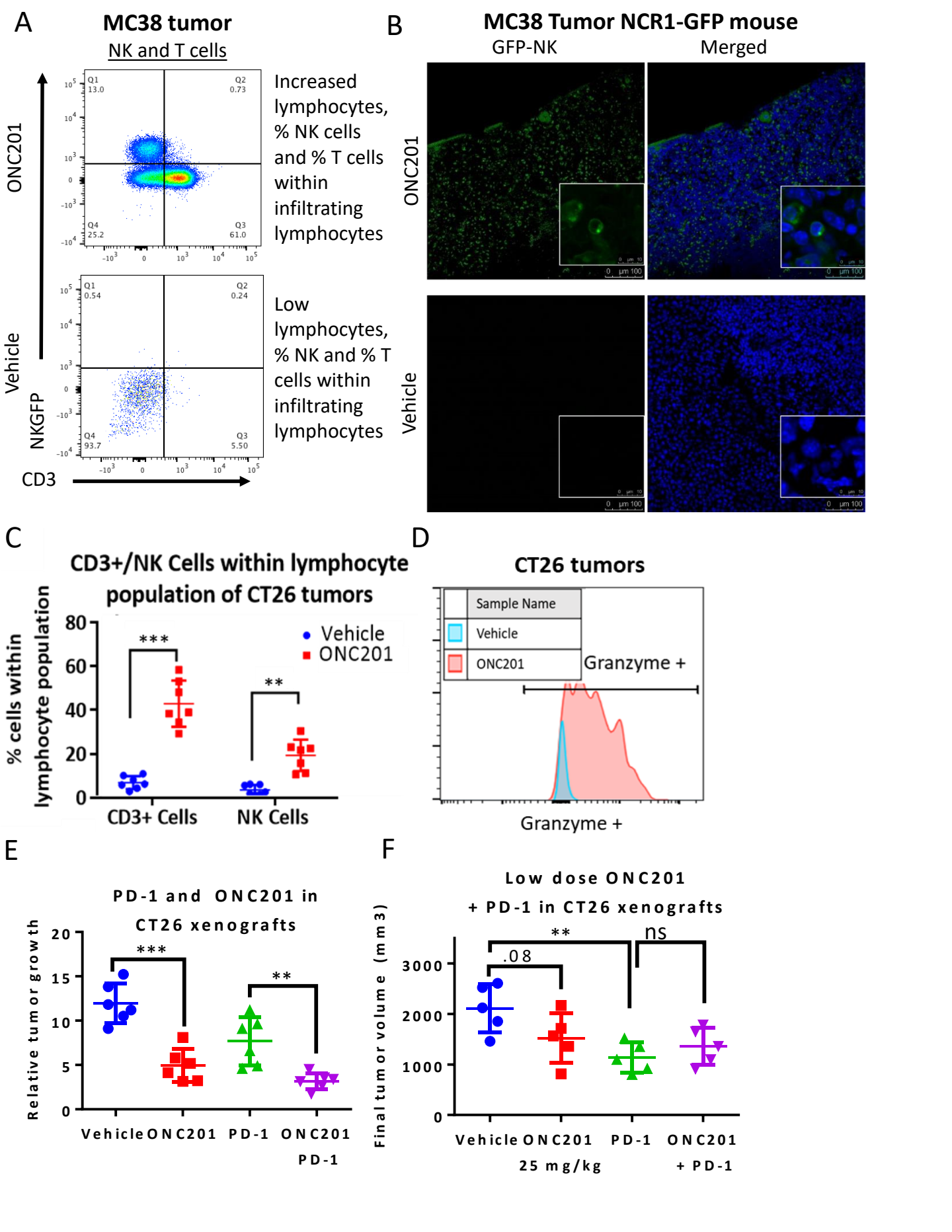

Wagner *et al.*, Figure 5

Figure 5: ONC201 induces NK accumulation and activation and CD4/CD8+ CD3+ T cell accumulation. (A) Analysis of NK and T cells in MC38 xenografts in NCR1-gfp mice. (B) Immunofluorescence of MC38 tumors in NCR1-GFP C57/BL6 mice of GFP-expressing tumors and DAPI using 20x and 100x magnification. (C) Comparison of T cell and NK cell population in CT26 tumors in Balb/c mice. (D) Analysis of NK cells and NK cell granzyme expression and MFI on CT26 tumors in Balb/c mice. (E) Relative tumor volume after 4 weeks in CT26 tumors in Balb/c mice treated with Vehicle, 100mg/kg ONC201, PD-1, or ONC201 + PD-1. (F) Final tumor volumes after 4 weeks in CT26 tumors in Balb/c mice treated with Vehicle, 25 mg/kg ONC201, PD-1, or ONC201 + PD-1. (For mouse studies: NCR-1-GFP mice N=4; CT26 PBMC experiment N=7, CT26 PD-1 100 mg/kg experiment in e n=7, CT26 PD-1 25 mg/kg experiment in f n=7). (P values are as indicated: **$p < 0.01$, *** $p < 0.001$, **** $p < 0.0001$ relative to vehicle using 2-sided Wilcoxon rank sum test). For immunofluorescence: Green: GFP, Blue: DAPI. Merge performed by Image J. Sections were performed on 4 sections per tumor, quantitation in supplemental. Data represent the mean +/- SD.

A

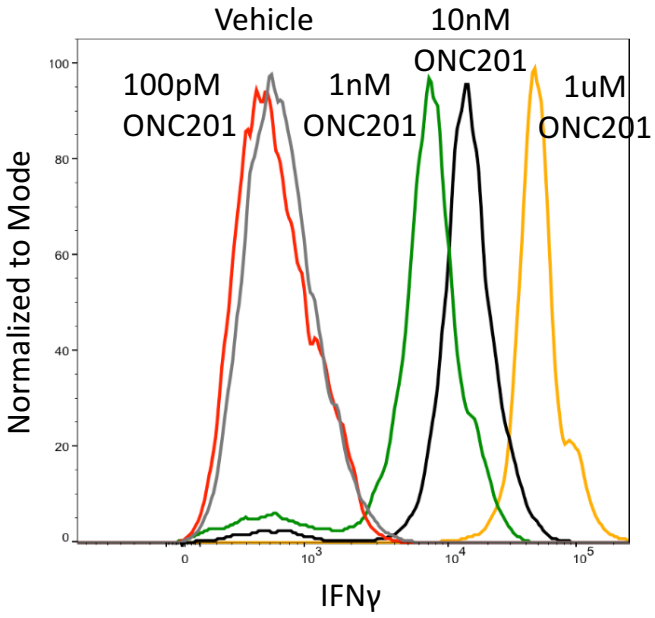

B

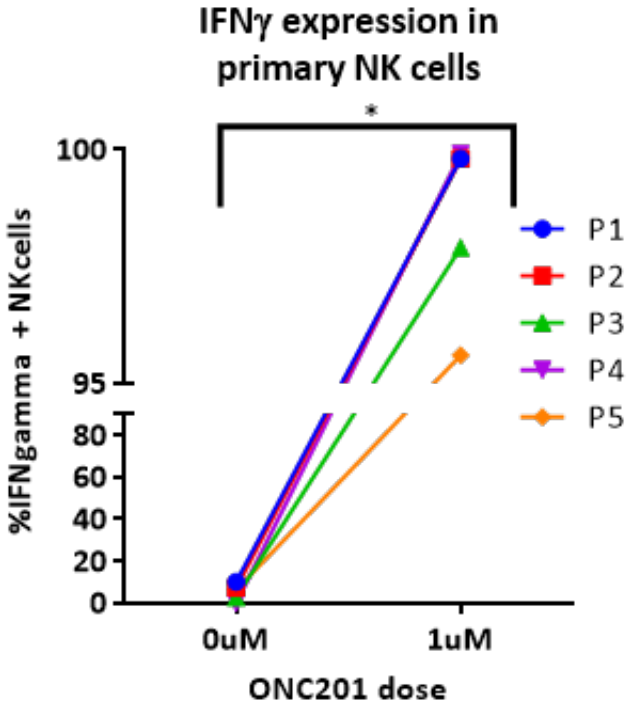

C

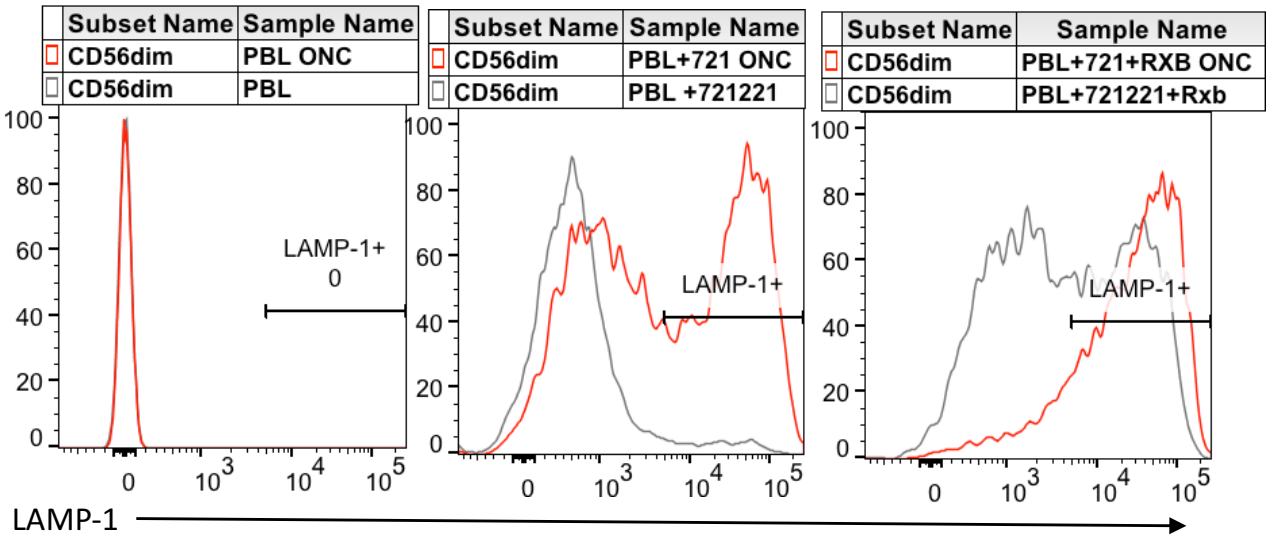

Wagner *et al.*, Figure 6

Figure 6: ONC201-induces primary NK cell activation and de-granulation. (A) Human primary NK cell IFNγ titration within increasing doses of ONC201 (B) Analysis of 5 healthy donors using 1μM ONC201 treatment (C) LAMP1+ Expression in the absence/presence of target cells using vehicle or 1uM ONC201 treatment. Cells treated overnight in ONC201 or vehicle. (For healthy human samples N=5). (P values are as indicated: * $p < 0.05$ relative to vehicle using 2-sided Wilcoxon rank sum test). Data represent the mean +/- SD.

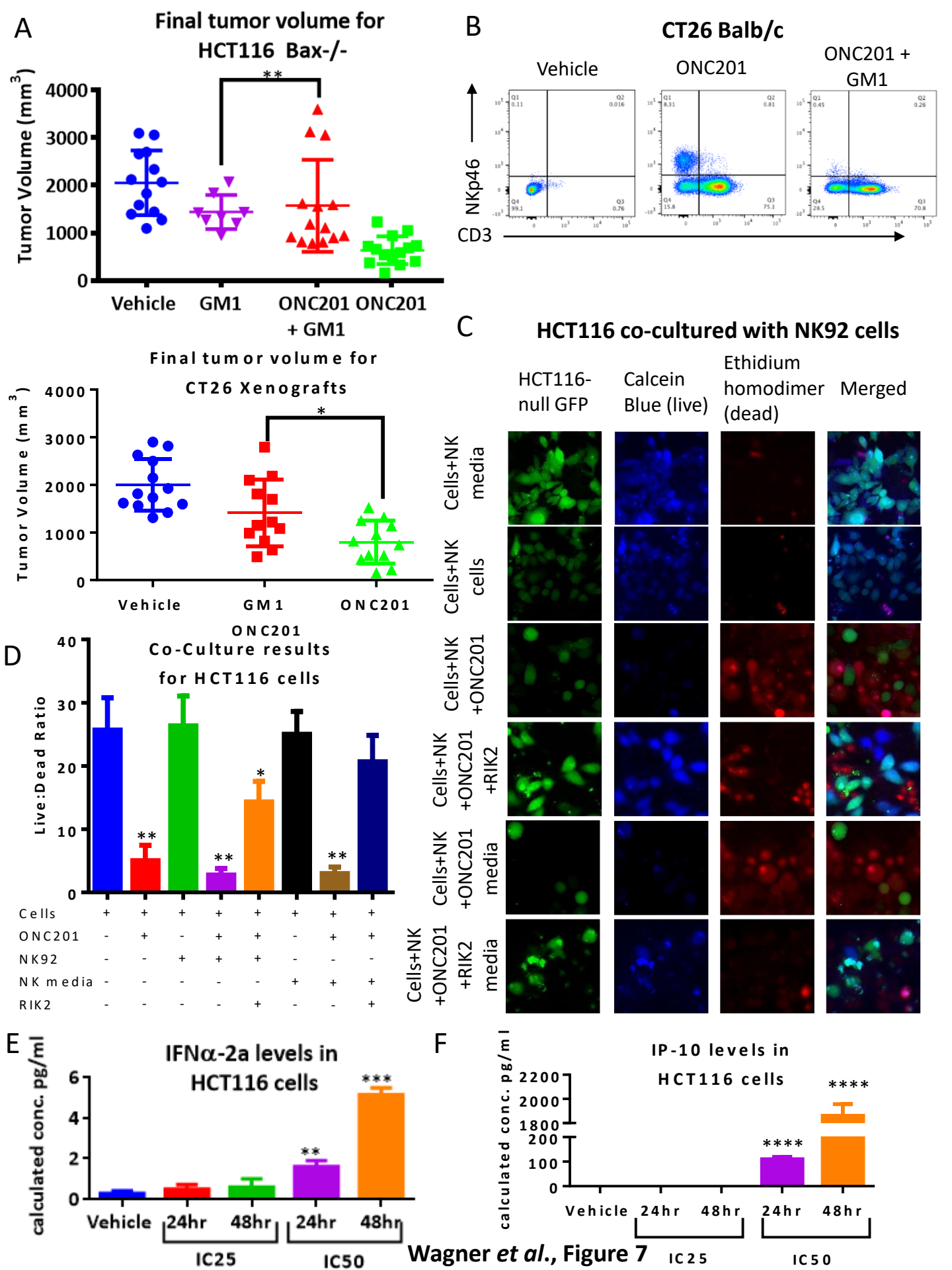

Wagner *et al.*, Figure 7

Figure 7: ONC201-induced NK activation/accumulation plays an important role in anti-tumor effect. (A) Final tumor volumes of *Bax*$^{-/-}$ (top) and CT26 (bottom) with 100 mg/kg ONC201 weekly for 4 weeks and GM1 every 5 days as prescribed. (B) NK cells enrichment by ONC201 and depletion by GM1 are confirmed with flow cytometry in the CT26 bearing mice. (C) Fluorescence microscopy from co-culture of HCT116 *p53*$^{-/-}$-GFP and NK cells or NK media treated as indicated for 48 hours. (D) Quantitation of fluorescence microscopy. Multiplex analysis of data of (E) IP-10 and (F) IFNα-2a levels within conditioned media from ONC201 treated HCT116 cells. More shown in supplemental. ONC201 10 μM, RIK2 2 mg/ml. Green: GFP, Blue: Calcein AM, Red: PI. Merge performed by Image J. Non-gfp blue+ cells are NK cells. Flow cytometry performed on PI+ CD19-/CD45+ cells (For mice, N=10 for CT26 and *Bax*$^{-/-}$ GM1 studies. For co-cultures, n=3 and where ran separately twice. For multiplex, n=3 ran in duplicate (6 samples total)). (P values are as indicated ** $p < 0.01$, *** $p < 0.001$, **** $p < 0.0001$ compared to vehicle using 2-sided Wilcoxon rank sum test, for multiplex ELISA study, three separate conditioned media samples per cohort where harvested and ran in duplicate. The mean of each duplicate was taken and compared using a 2-sided Wilcoxon rank sum test). Data represent the mean +/- SD.

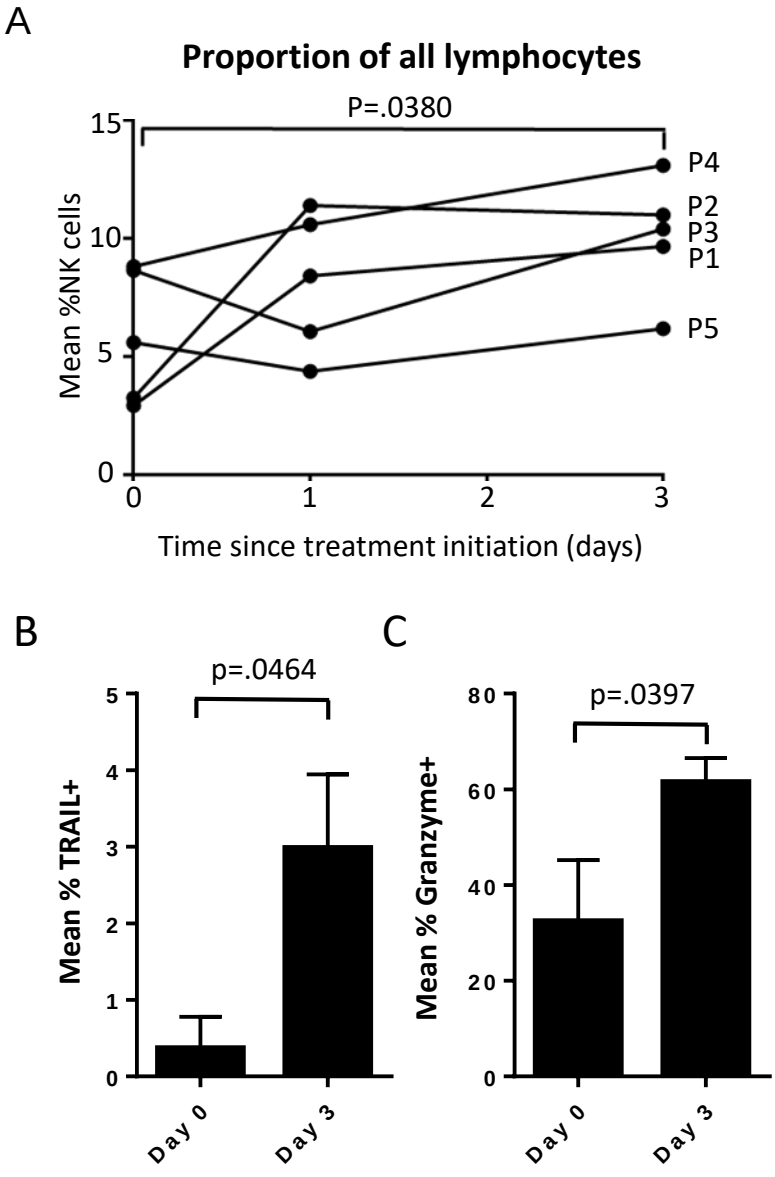

Wagner *et al.*, Figure 8

Figure 8: NK cells are increased in peripheral blood of patients following treatment with ONC201. (A) Percentage of NK cells expressing TRAIL. (B) Percentage of NK cells expressing Granzyme B. P value as indicated for Day 3 vs Day 0. P values are as indicated compared to Day 0 using a paired 2-sided t test. Data represent the mean +/- SD.